The Laminar-Turbulent Transition in Nonisothermal Flow of Pseudoplastic Fluids in Tubes

RICHARD W. HANKS and E. B. CHRISTIANSEN

University of Utah, Salt Lake City, Utah

Ryan and Johnson's treatment of the transition from laminar to turbulent flow is extended to include the heated flow of pseudoplastic liquids in smooth tubes. A limitation is pointed out for the case of Bingham plastic fluids.

The theoretical results of the present investigation are compared with experimental data obtained for a large number of pseudoplastic fluids having widely variant rheological properties. It is found that the theoretically predicted flow rates corresponding to the inception of turbulence agree with the observed values to within ± 6.7%. The theoretical critical wall shear stresses agree within ± 3.87% with experiment.

PREVIOUS RESEARCH

The standard criterion for stability of laminar flow of Newtonian fluids in pipes is the value 2,100 of the Reynolds number. Ryan and Johnson (*1*) have treated the problem of laminar flow stability in general and proposed a more general criterion for flow stability of which the ordinary Reynolds number is a special case.

They tested their parameter for the case of isothermal pipe flow of pseudoplastic fluids (*1*) and showed it to be valid for power-law fluids. They were also able to predict the correct radial position at which maximum instability occurs for the isothermal tube flow of Newtonian fluids.

No criterion is available in the literature for predicting the transition from laminar to turbulent flow for the nonisothermal flow of pseudoplastic fluids. For nonisothermal Newtonian flow the familiar empirical Sieder-Tate correlation (*2*) may be used with reasonable accuracy.

The present paper will generalize the method of (*1*) for predicting the onset of turbulence to include the heated flow of pseudoplastic liquids in smooth round tubes.

THEORETICAL ANALYSIS

The stability criterion (*1*) is

$$Z_j = -\frac{\rho R_w}{g_c \tau_w} u \left(\frac{du}{dr}\right) \qquad (1)$$

If r is replaced by $x = r/R_w$, Equation (1) may be written as:

$$Z_j = -\frac{\rho}{g_c \tau_w} u \left(\frac{du}{dx}\right) \qquad (2)$$

It was suggested (*1*) that when a laminar flow field is sufficiently unstable to become turbulent, Z_j would exhibit at some point in the cross section a maximum value which was numerically equal to 808.

If Equation (2) is differentiated with respect to x and the resultant derivative set equal to zero (the necessary condition that Z_j be extremal), the following nonlinear differential equation is obtained:

$$-u\left(\frac{d^2u}{dx^2}\right) = \left(\frac{du}{dx}\right)^2 \qquad (3)$$

The root x_c of Equation (3) is the point at which the flow field exhibits its maximum instability and where turbulence will most probably be initiated by a random disturbance. It was shown (*1*) that the isothermal solution to Equation (3) for power-law rheology is

$$x_{oj} = \left[\frac{1}{2+n}\right]^{\frac{n}{1+n}} \qquad (4)$$

where n is the exponent of the empirical Ostwald-deWaele or power-law equation

$$\tau = K\left(\frac{du}{dr}\right)^n \qquad (5)$$

Equation (5) is a convenient two-constant equation which has been found to afford a reasonable fit of rheological data for many non-Newtonian fluids. For constant values of n and K Equation (5) may be written in the equivalent form for tube flow

$$\tau_w = K'\left[\frac{Q}{\pi R_w^3}\right]^n \qquad (6)$$

where

$$K' = K\left[\frac{1+3n}{n}\right]^n \qquad (7)$$

From Equations (4), (5), and (2) one obtains

$$\tau_{wc} = \frac{\rho R_w^2}{808 g_c} \frac{(1+3n)^2}{n} \left[\frac{1}{2+n}\right]^{\frac{2+n}{1+n}} \Gamma^2 \qquad (8)$$

where $\Gamma \equiv Q/\pi R_w^3$. Equation (8), when written in logarithmic form

$$\ln \tau_{wc} = 2 \ln \Gamma + \ln\left[\frac{\rho R_w^2}{808 g_c}\right] + \ln\left\{\frac{(1+3n)^2}{n}\left[\frac{1}{2+n}\right]^{\frac{2+n}{1+n}}\right\} \qquad (9)$$

shows that a plot of Equation (8) on logarithmic coordinates yields a straight line with a positive slope of two. The critical values of τ_w and Γ correspond to the coordinates of the point of intersection of Equations (8) and (6) on a logarithmic plot. The authors shall now proceed to generalize the above results to include the heated flow of pseudoplastic liquids.

THE EFFECT OF TEMPERATURE ON $Z_{j\,max}$

In order to extend the above isothermal equations to include heated flow one must be able to specify the value of $Z_{j\,max}$ for various temperature profiles. Several observations may be cited to substantiate the assumption that $Z_{j\,max}$ is not effected by heating.

The general effect of heating a fluid in laminar motion is to blunt its velocity profile (*4*). The same effect on the velocity profile is caused by increasing the degree of pseudoplasticity (smaller values of n) (*3, 5*). Therefore the effect of heating on $Z_{j\,max}$ should be quite similar to the effect of decreasing the value of n. This latter effect may be readily examined experimentally. In Figure 1 experimental values of isothermal critical friction factor taken from the literature are plotted as a function of n. The curve shows Ryan and Johnson's theoretical values of the critical friction factor and is based on the assumption of a constant

R. W. Hanks is with Union Carbide Nuclear Company, Oak Ridge Gaseous Diffusion Plant, Oak Ridge, Tennessee.

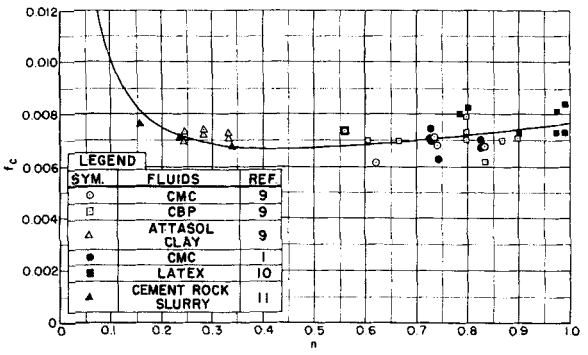

Fig. 1. Comparison of Johnson's predicted f_c with data for pseudoplastic fluids.

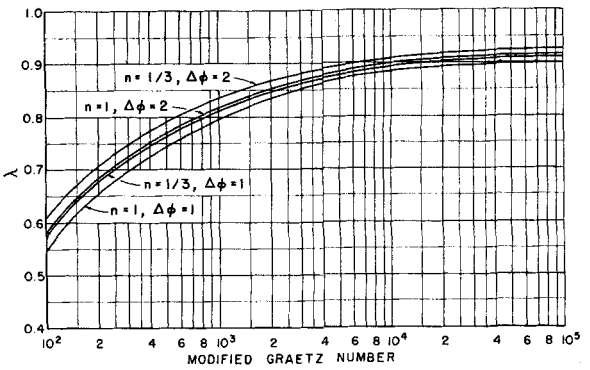

Fig. 2. Nonisothermal laminar flow parameter λ.

value of $Z_{j\ max} = 808$. The agreement between their predictions and the experimentally observed values of f_c is essentially exact from $n = 0.16$ to unity. This fact indicates that $Z_{j\ max}$ is essentially independent of the shape of the velocity profile, and hence one may infer that it might also be independent of the temperature profile.

Additional experimental justification of the assumption of the temperature independence of $Z_{j\ max}$ is found in the observations of Keevil and McAdams (7). These authors obtained data for cooling and heating of viscous Newtonian oils and observed that the friction factor-Reynolds number curves for their nonisothermal data were simply displaced vertically up or down from the usual isothermal curve. This observation suggests that for Newtonian fluids the critical Reynolds number is essentially independent of temperature gradients. Since $Z_{j\ max}$ is a constant times the Reynolds number, it follows that it also must be independent of the temperature profile for Newtonian fluids. Therefore, since $Z_{j\ max}$ $(n = 1)$ is independent of the temperature profile, and since $Z_{j\ max}$ (n) is apparently independent of n, it seems quite probable that $Z_{j\ max} = 808$ is a unique constant which is characteristic of the inception of turbulence, at least in tube flow of power-law pseudoplastic and Newtonian fluids, and is independent of the temperature level or the existence of temperature gradients in the flow field. This constant maximum value of the stability parameter shall therefore be used in the following derivations.

NONISOTHERMAL FLOW TRANSITION

The existence of a steady state nonisothermal flow field in fully developed laminar motion which is approaching the condition of maximum instability with respect to flow perturbations is assumed. It is also assumed that the rheological behavior of the fluids being considered is fully described by the reduced Ostwald-deWaele (3, 6, 8) or power-law Equation:

$$\tau = k_\sigma \left\{ \frac{du}{dr} \exp\left[\phi(r)\right] \right\}^n \quad (10)$$

where

$$\phi(r) = E^\ddagger / RT(r) \quad (11)$$

By means of Equation (10) one may rewrite Equations (3) and (8) as follows:

$$\int_{x_c}^1 (x)^{1/n} \exp\left[-\phi(x)\right] dx =$$

$$\frac{(x_c)^{\frac{1+n}{n}} \exp\left[-\phi(x_c)\right]}{\frac{1}{n} - x_c \left.\frac{d\phi(x)}{dx}\right|_{x=x_c}} \quad (12)$$

and

$$\tau_{wc} = \frac{\rho R_w}{808 g_c}$$

$$\frac{(x_c)^{\frac{2+n}{n}} \exp 2[\phi_i - \phi(x_c)]}{\frac{1}{n} - x_c \left.\frac{d\phi(x)}{dx}\right|_{x=x_c}} \frac{\Gamma^2}{4I_q^2} \quad (13)$$

where

$$I_q = \int_o^1 x \int_x^1 (\xi)^{1/n} \exp\left[\phi_i - \phi(\xi)\right] d\xi\, dx \quad (14)$$

Just as in the isothermal case, the critical values of τ_w and Γ are given by the simultaneous solution of Equations (13) and (10) (rearranged into a form involving τ_w and Γ as variables). The value of x_c to be used in Equation (13) is obtained by solution of Equation (12).

The indicated integrations may be performed analytically if a mathematically tractable function $\phi(x)$ is available. A relatively convenient and simple form of $\phi(x)$ proposed by the authors (3, 8) may be described by the following set of equations:

$$\phi(x) = \phi_i = \text{constant}; \quad 0 \leqq x \leqq \lambda$$

$$\phi(x) = \phi_w + \frac{\Delta\phi}{\ln \lambda} \ln x; \quad \lambda \leqq x \leqq 1 \quad (15)$$

$$\Delta\phi \equiv \phi_i - \phi_w = \frac{E^\ddagger}{R}\left[\frac{1}{T_i} - \frac{1}{T_w}\right]$$

The parameter λ is a function of the Graetz number and was determined from numerical solutions of the heat conduction equation for laminar flow of fluids (3, 8). This function is shown graphically in Figure 2. The abscissa is a modified form of the Graetz number defined as $N_{Gz}' = \dot{m}C/kL$.

The value of x_c for which Equation (12) is satisfied might possibly be less than, equal to, or greater than the value of λ. By considering the limiting values of x_c for these various possibilities, one may show that the correct solution corresponds to the case $x_c > \lambda$.

The possibility of equality of x_c and λ is excluded because of the discontinuity in the first derivative of $\phi(x)$

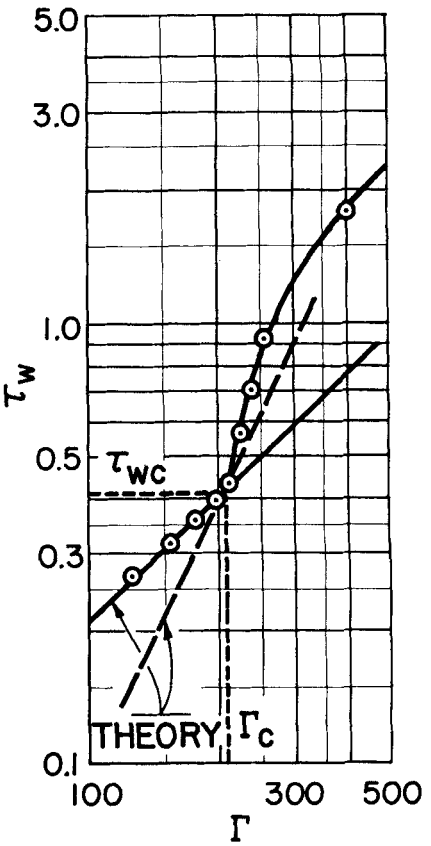

Fig. 3. Comparison of theoretical curves with data for CMC-C solution.

at the point $x = x_c$. Consideration of the possibility of $x_c < \lambda$ immediately leads one to unpermissible limiting values.

The limiting conditions which shall be examined are the following:

1. Isothermal flow ($\Delta\phi = 0$).
2. Plug flow ($\Delta\phi = \infty$).
3. Infinite flow rate ($N_{Gz}' = \infty$ or $\lambda = 1$).
4. Infinite heated length ($N_{Gz}' = 0$ or $\lambda = 0$).

For $\lambda < x_c$ the root of Equation (12) is found (3) to be

$$x_{ch} = \frac{f(n)}{1 + 2f(n)} \frac{1}{1 + f(n)} \quad (16)$$

where

$$f(n) = \frac{1}{n} - \frac{\Delta\phi}{\ln \lambda} \quad (16a)$$

An equivalent form of Equation (16) is

$$x_{ch} = \left\{ \frac{\ln \lambda - n\Delta\phi}{(2 + n) \ln \lambda - 2n\Delta\phi} \right\}^{\frac{n \ln \lambda}{(1 + n) \ln \lambda - n\Delta\phi}} \quad (17)$$

from which the following limits may readily be deduced:

$$\lim_{\Delta\phi \to 0} x_{ch} = x_{cj} \quad (18a)$$

$$\lim_{\Delta\phi \to \infty} x_{ch} = 1 \quad (18b)$$

$$\lim_{\lambda \to 1} x_{ch} = 1 \quad (18c)$$

$$\lim_{\lambda \to 0} x_{ch} = x_{cj} \quad (18d)$$

The above limits are consistent with the initial assumption of $\lambda < x_c$. The limit $\Delta\phi = 0$ corresponds to isothermal flow, and Equation (17) reduces to Equation (4). The limit shown as Equation (18*b*) corresponds to plug flow. For plug flow the local velocity is everywhere constant in the cross section, and the shear rate is everywhere zero except at the wall, ($x = 1$), where it is infinite. Hence the extremal value of Z_j must occur at $x = 1$. The limit shown in Equation (18*c*) is a necessary result of the assumption $\lambda < x_c$. The limit shown in Equation (18*d*) corresponds to an infinitely long heated length in which the fluid approaches the temperature of the wall, wherein the isothermal results must again apply. Consequently Equation (16) represents the correct solution to Equation (12). The task remaining is to test the results which may be derived from Equation (16) against experimental observations.

When Equation (16) is introduced into Equation (13) and the integral in Equation (14) is evaluated for the case $\lambda < x_c$, one has

$$\tau_{wc} = \frac{\rho R_w^2}{808 g_c} \frac{\exp[2\Delta\phi](x_{ch})^{r(n)} \left[\frac{1 + 3n}{n}\right]^2 \Gamma^2}{R(n, \Delta\phi, \lambda)} \quad (19)$$

where

$$r(n) = \frac{1 + 2f(n)}{1 + f(n)} \quad (20)$$

and

$$R(n, \Delta\phi, \lambda) = f(n) \left\{ \frac{\left(\frac{1 + 3n}{n}\right) \exp(\Delta\phi)}{3 + f(n)} [1 - \lambda^{3 + f(n)}] + \frac{(\lambda)^{\frac{1 + 3n}{n}}}{} \right\} \quad (21)$$

Equation (19) must be solved simultaneously with Equation (10) to obtain the values of τ_w and Γ corresponding to the onset of turbulence for the heated flow of pseudoplastic liquids.

EXPERIMENTAL RESULTS

The equipment used in the experimental portion of the present investigation has been described elsewhere (3, 8), and consequently no discussion of it will be presented here.

The above-mentioned simultaneous solution of Equations (19) and (10) is most easily accomplished graphically. For this purpose Equation (10) may be rewritten in the form

$$\tau_w = k_{\gamma i} \Gamma^n \zeta_f^{-n} \quad (22)$$

where

$$k_{\gamma i} = k_\sigma \left(\frac{1 + 3n}{n}\right)^n \exp(n\phi_i) \quad (23)$$

and

$$\zeta_f = \frac{R(n, \Delta\phi, \lambda)}{f(n)} \quad (24)$$

In Figures 3 through 6 graphical solutions of Equations (19) and (22) are compared with typical experimental data obtained in the present investigation for flow of aqueous solutions of carboxymethylcellulose and carbopol in smooth copper tubes. The solid lines designated *Theory* are plots of Equation (22); the dashed lines designated *Theory* are plots of Equation (19). The intersection of these two curves should be coincident with the break point of smooth curves drawn through the experimental points. The success of the theoretical predictions is obvious from these plots. Figure 8 is a quantitative comparison of the predicted critical value of Γ with the experimentally observed value. The results are correlated with a mean deviation of ± 6.7%. Figure 7 is a similar comparison for the critical wall shear stresses which are correlated with a mean deviation of ± 3.87%. Table 1 shows the maximum ranges of variables covered in the present experimental work. Table 2 contains a tabulation of the important experimental results of the present work.

In view of the inherent uncertainties involved in nonisothermal transitional flow data, the 6.7% mean deviation obtained in Figure 8 and the 3.87% deviation shown in Figure 7 are considered to be excellent.

The results of the theoretical analysis apply to fluids whose rheology can be represented by the empirical power-law and under conditions such that the temperature profile is represented by

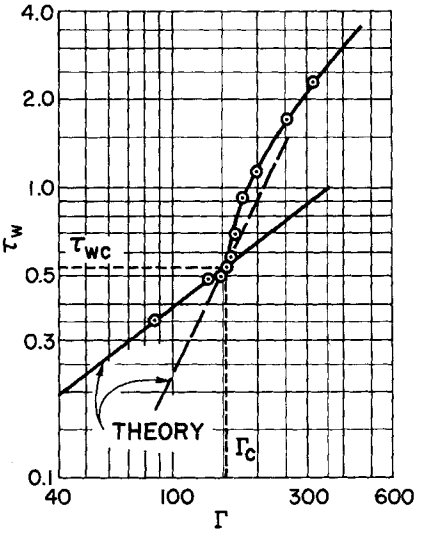

Fig. 4. Comparison of theoretical curves with data for CMC-E solution.

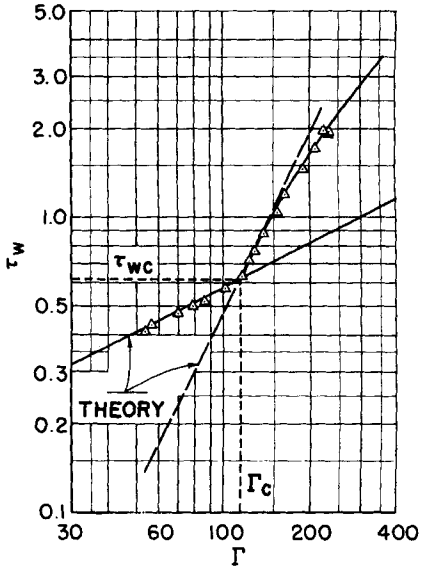

Fig. 5. Comparison of theoretical curves with data for CBP-E solution.

Table 1. Experimental Conditions Covered

Variable	Range of values
n	0.498 to 0.936
$\Delta\phi$	0.527 to 1.630
D	1.063, 1.600, 2.063 in.
ΔT	18.6 to 50.2°C.
L/D	28 to 215
ζ_f"	1.106 to 1.700

Table 2. Important Experimental Results

Fluid	n	lb.$_f$ sec.^{n}/sq. ft. $10^7 k_\sigma$	°K. $E^\ddagger/R$	°C. ΔT_{av}	lb.$_f$/sq. ft. τ_{wc} (exp)	sec.$^{-1}$ Γ_c (exp)
CMC-B	0.923	3.841	2,836	26.5	—	—
C	0.936	1.041	3,190	48.5	0.420	212
D	0.740	22.14	3,540	43.3	0.800	192
E	0.751	19.61	3,450	38.9	0.550	162
F	0.800	18.58	3,147	31.0	0.434	139
G	0.756	86.28	2,791	36.3	0.870	298
H	0.819	2.439	3,750	35.8	0.209	69
I	0.800	4.683	3,587	36.1	0.199	71
J	0.600	86.57	4,497	31.1	1.600	300
K	0.657	219.8	3,115	28.7	0.580	158
CBP-A	0.526	2,122	2,717	37.0	0.425	138
B	0.584	1,140	2,510	43.0	0.440	190
E	0.498	2,763	3,073	40.6	0.622	118
F	0.582	725.8	2,920	40.3	0.450	128
G	0.503	9,037	2,619	38.8	1.580	238
H	0.561	6,944	2,051	41.3	1.280	320

an empirical (but apparently quite satisfactory) approximation. Despite this limitation on the rigor of their origin however the theoretical equations derived above agree satisfactorily with experimental observations. The authors feel that the reliability of these results has been adequately demonstrated and that the equations herein proposed may be used with confidence to predict the onset of turbulence in the heated flow of pseudoplastic liquids in smooth round tubes. This prediction may be made from only a knowledge of the rheological constants of the fluid and the physical specifications of the system.

It should be pointed out here that the present analysis applies equally well to Newtonian liquids, the only requirement being a simple exponential dependence of viscosity on temperature. Unfortunately some of the common Newtonian fluids do not exhibit this type of viscosity temperature relation, and hence in such cases the results of this paper cannot be applied.

NOTATION

C = heat capacity of liquid
$E^\ddagger$ = energy of activation for viscous flow
$f(n)$ = function defined by Equation (16a)
g_c = force unit conversion factor
I_q = integral defined by Equation (14)
k = thermal conductivity of liquid
$k_{\gamma i}$ = rheological constant defined by Equation (23)
k_σ = rheological constant defined by Equation (10)
K = power law consistency factor
K' = rheological constant defined by Equation (7)
L = length of heater
$\dot{m}$ = mass flow rate
n = power law exponent
N_{Gz}' = modified Graetz number, $\dot{m}C/kL$
Q = volumetric flow rate
r = radial position coordinate
R = gas law constant
$R(n, \Delta\phi, \lambda)$ = function defined by Equation (21)
R_w = radius of pipe
$r(n)$ = function defined by Equation (20)
T = absolute temperature
T_i = inlet temperature
T_w = wall temperature
u = local axial velocity component
x = normalized radial coordinate, r/R_w
x_{ch} = nonisothermal critical radius, Equation (16) or (17)
x_{cj} = isothermal critical radius, Equation (4)
Z_j = Johnson's stability parameter defined by Equation (1)

Greek Letters

Γ = pseudo shear rate, $Q/\pi R_w^3$
ζ_f = laminar nonisothermal flow function, Equation (24)
λ = nonisothermal flow parameter, Figure 2
π = 3.14159 . . . .
ρ = liquid mass density
τ = shear stress
τ_w = wall shear stress
τ_{wc} = critical wall shear stress
$\phi(r)$ = temperature profile function, $E^\ddagger/RT(r)$
ϕ_i = $E^\ddagger/RT_i$
ϕ_w = $E^\ddagger/RT_w$
$\Delta\phi$ = $\phi_i - \phi_w$

LITERATURE CITED

1. Ryan, N. W., and M. M. Johnson, *A.I.Ch.E. Journal*, **5**, 433 (1959).
2. Sieder, E. N., and G. E. Tate, *Ind. Eng. Chem.*, **28**, 1429 (1936).
3. Hanks, R. W., Ph.D. thesis, Univ. Utah, Salt Lake City, Utah (1960).

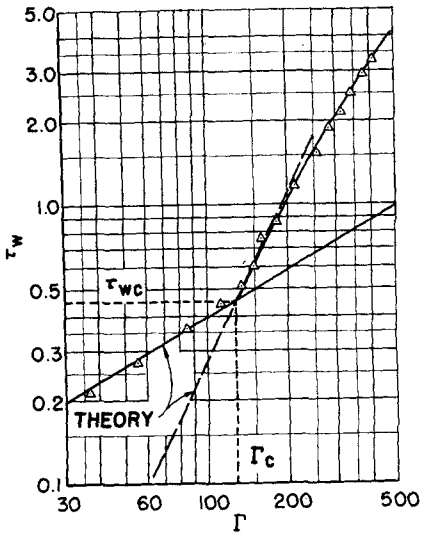

Fig. 6. Comparison of theoretical curves with data for CBP-F solution.

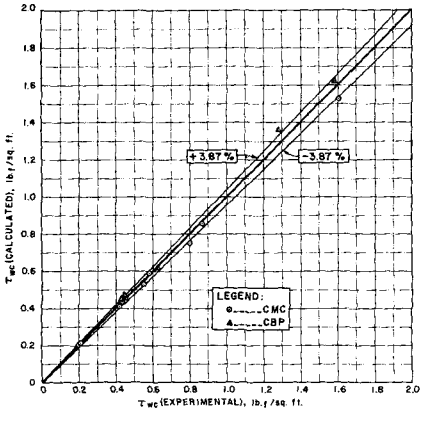

Fig. 7. Comparison of calculated and observed critical wall shear stresses.

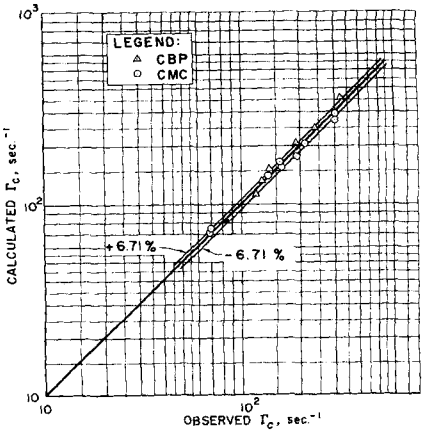

Fig. 8. Comparison of calculated and observed nonisothermal critical flow parameters Γ_c.

4. McAdams, W. H., "Heat Transmission," 3 ed., McGraw-Hill, New York (1954).
5. Dodge, D. W., and A. B. Metzner, *A.I.Ch.E. Journal*, **5**, 189 (1959).
6. Christiansen, E. B., and S. E. Craig, Jr., *ibid.*, **8**, 154 (1962).
7. Keevil, C. S., and W. H. McAdams, *Chem. & Met. Eng.*, **36**, 464 (1929).
8. Hanks, R. W., and E. B. Christiansen, *A.I.Ch.E. Journal*, **7**, 519 (1961).
9. Dodge, D. W., Ph.D. thesis, Univ. Del., Newark, Delaware (1957).
10. Winding, C. C., W. L. Kranich, and G. P. Bowman, *Chem. Eng. Progr.*, **43**, 613 (1947).
11. Wilhelm, R. H., D. M. Wroughton, and W. L. Loeffel, *Ind. Eng. Chem.*, **31**, 622 (1939).
12. Thomas, D. G., Paper presented at Am. Inst. Chem. Engrs. Meeting, Salt Lake City, Utah (September, 1958).
13. *Proc. Am. Soc. Civil. Engrs.*, **55**, 1773 (1929).
14. Govier, G. W., and M. D. Winning, Paper presented at Am. Inst. Chem. Engrs., Meeting, Montreal, Canada (September, 1948).
15. Alves, G. E., D. F. Boucher, and R. L. Pigford, *Chem. Eng. Progr.*, **48**, 385 (1952).
16. Gregory, W. B., *Mech. Eng.*, **49**, 609 (1927).
17. Merkel, W., *Beschefte zum Gesundheits Ing.*, Reihe II, Heft 14 (1934).
18. Caldwell, D. W., and H. E. Babbitt, *Trans. Am. Inst. Chem. Engrs.*, **37**, 237 (1941); *Ind. Eng. Chem.*, **33**, 249 (1941).
19. Stevens, W. E., Ph.D. thesis, Univ. Utah, Salt Lake City, Utah (1952).
20. Metzner, A. B., and J. C. Reed, *A.I.Ch.E. Journal*, **1**, 434 (1955).

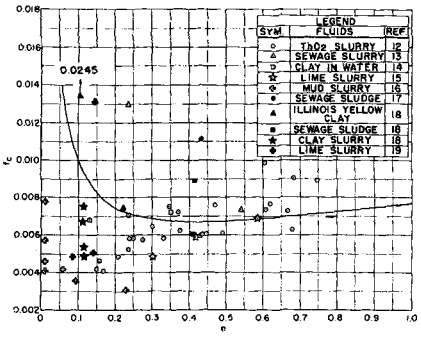

Fig. 9. Comparison of Johnson's isothermal critical friction factor equation with Bingham plastic data.

Manuscript received August 22, 1961; revision received December 5, 1961; paper accepted December 5, 1961. Paper presented at A.I.Ch.E. New York meeting.

APPENDIX

Bingham Plastic Fluids

Figure 9 is a plot similar to Figure 1 showing a comparison of experimental critical friction factors (obtained from the literature for fluids conforming reasonably well to the Bingham plastic model) with a curve calculated by Ryan and Johnson (*1*). The values of n used in plotting the experimental points were obtained from tangents drawn to the laminar flow curve (plotted on logarithmic paper) at the break point in accord with the method suggested by Metzner and Reed (*20*).

It is quite evident that the data shown in Figure 9 do not agree quantitatively or qualitatively with the computed curve. This observation emphasizes the fact that the parameter n, the point slope of the log-log plot of experimental τ_w-Γ data, is not a general rigorous index of the flow process except in the case of a true power-law fluid. In the case of Bingham plastic fluids one might expect the presence of the unsheared plug in the central region of the pipe to contribute significantly to the stability of the flow field. Since Metzner and Reed's technique for treating all fluids in terms of a generalized power law fails to take into account the semisolid properties of the plastic fluids, one must conclude that their method is inapplicable to these fluids. Thus in predicting the onset of turbulence for non-Newtonian fluids it has been shown that one cannot apply a combination of Ryan and Johnson's theoretical treatment in terms of the power law with Metzner's point slope technique. Further theoretical investigation of this problem is thus seen to be needed.

Maximum Stable Drop Size in Turbulent Flow

C. A. SLEICHER, JR.

Shell Development Company, Emeryville, California

PURPOSE AND SCOPE

Two or more liquids may be caused to flow together in a pipe for the purpose of dissolving the liquids, transferring a third component from one phase to the other, carrying out a chemical reaction, or simply transporting both liquids from one place to another. Whatever the purpose it is often desirable to know something about the sizes of drops that are formed in the pipe. Knowledge of some kind of average size is often sufficient, although sometimes the distribution of sizes is required. This paper concerns the upper limit of stable drop size, knowledge of which is useful for several reasons. First of all the maximum stable drop size d_{max} can itself be used in place of the average drop size for making conservative estimates of mass transfer rates. Secondly, under some conditions, it may be possible to relate an average drop size to d_{max}. Indeed failure to take into account the existence of an upper limit in estimates of a drop size distribution function may lead to considerable error (*7*). Finally knowledge of d_{max} and the way in which drops are broken in a pipe may be valuable for comparison with results of theories of turbulence.

Presented here are the results of an investigation of the largest stable drop size that can exist in the turbulent pipe flow of two immiscible liquids. The two principal limitations of the experimental work are that pipe of only 1 diam. was used and that the volume fraction of the dispersed phase was always very low. The Reynolds numbers of the flow of the continuous phase varied from 8,900 to 78,000, and the range of other variables may be seen in Table 4.

EXPERIMENTAL EQUIPMENT AND ITS OPERATION

A schematic diagram of the basic apparatus is shown in Figure 1. In order to minimize the quantity of contaminants in the system the 1½-in. galvanized iron

C. A. Sleicher, Jr. is at the University of Washington, Seattle, Washington.